iScience, Volume *26*

Supplemental information

Single-cell RNA sequencing uncovers dynamic roadmap and cell-cell communication during buffalo spermatogenesis

Liangfeng Huang, Junjun Zhang, Pengfei Zhang, Xingchen Huang, Weihan Yang, Runfeng Liu, Qinqiang Sun, Yangqing Lu, Ming Zhang, and Qiang Fu

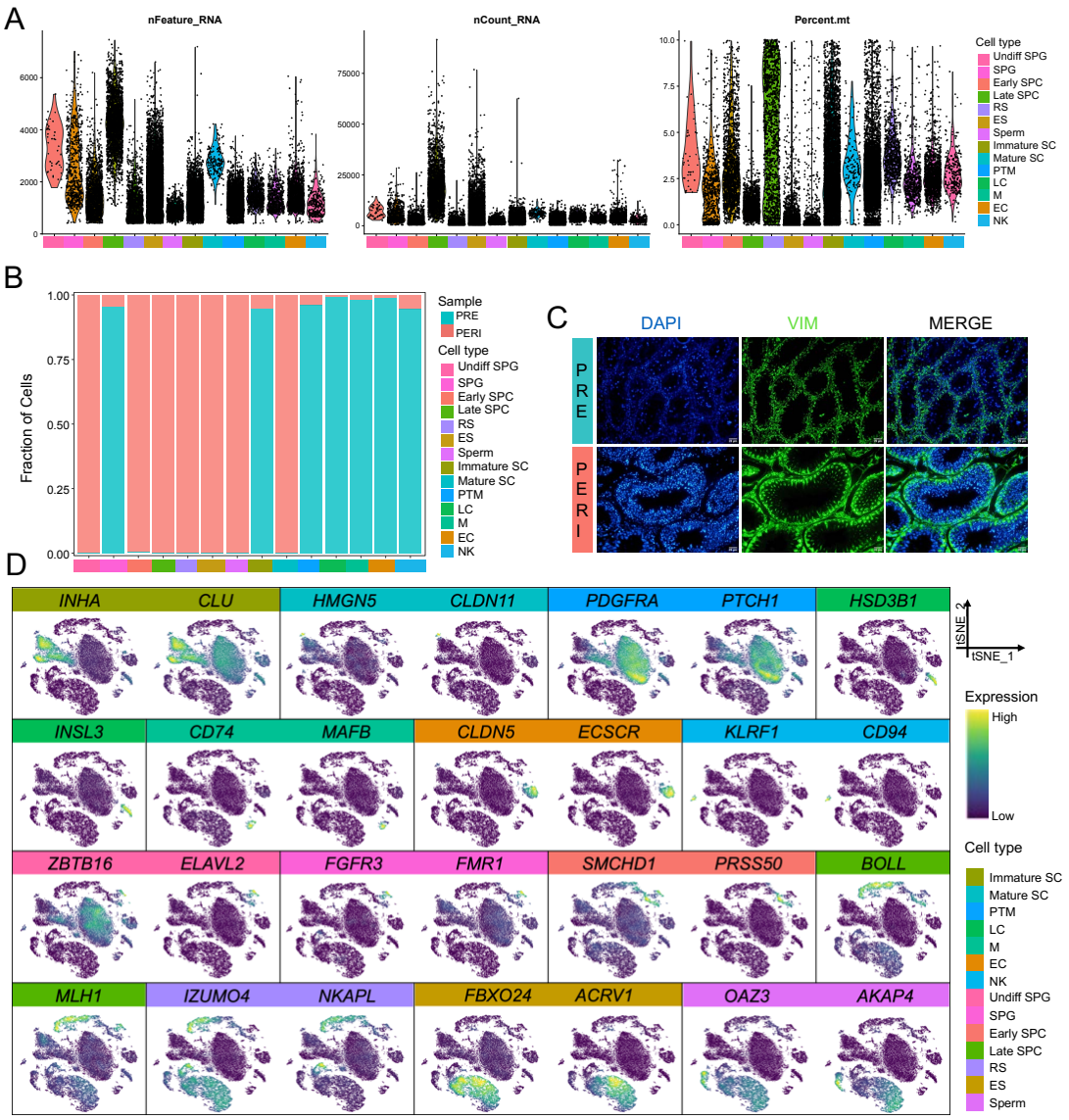

Figure S1. Identification of buffalo male testicular cells and quality control of scRNA-seq data, related to Figure 1. (A) Number of genes maintained after quality control (left), number of UMIs (middle), and percentage of mitochondrial genes (right). (B) The percentage stacked bar plot shows the proportion of cells derived from each testis used in this study. (C) IF analysis of antibody staining against VIM on paraffin sections of prepubertal and pubertal buffalo testes. Scale bar, 20 μm. (D) Expression patterns of selected markers projected on the tSNE plot.

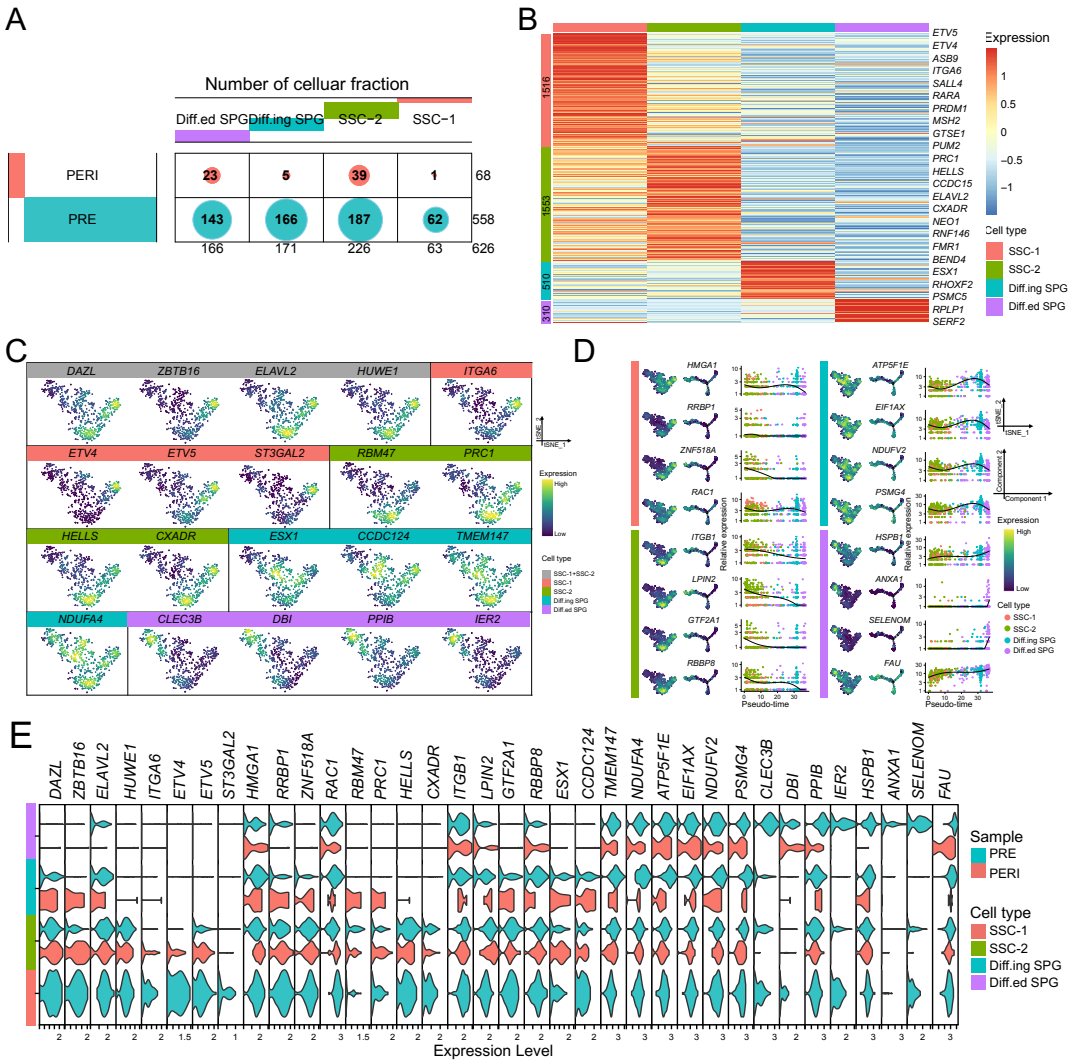

Figure S2. Dynamic gene expression pattern analysis of SPG subsets, related to Figure 2. (A) Balloon plot showing the number of cellular fractions in SPG subsets. (B) Heatmap of normalized expression in the DEGs (Wilcoxon rank sum test, p-value < 0.05) of SPG subsets. (C) Expression patterns of additional markers projected on the tSNE plot. (D) Feature plots, trajectory plots, and pseudotime trajectory expression patterns of additional markers in SSC-1, SSC-2, Diff.ing SPG and Diff.ed SPG. (E) Violin plot of additional gene expression split by sample.

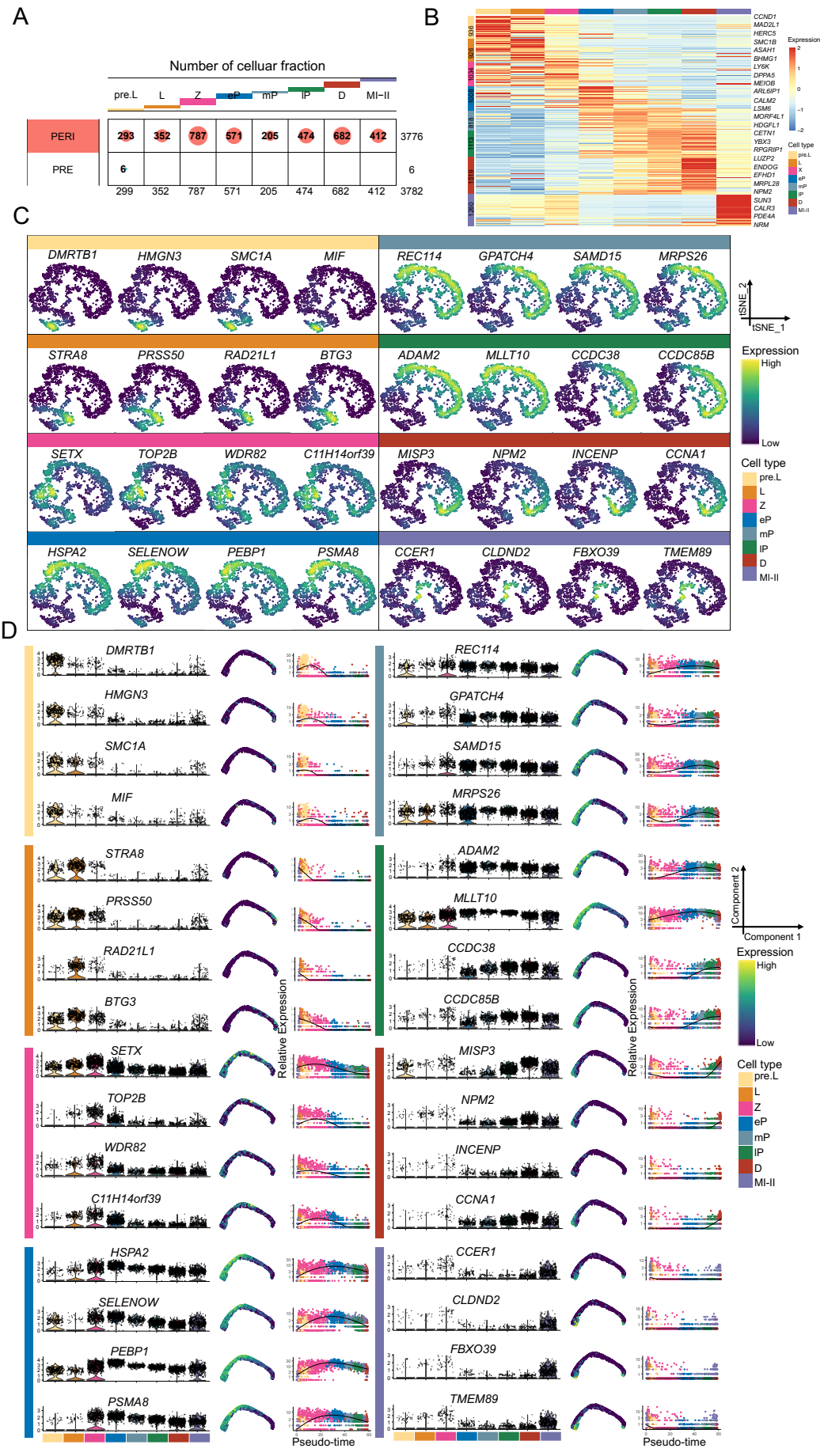
A
Number of celluar fraction
pre.L
L
Z
eP
mP
IP
D
MI−II
PERI
293
352
787
571
205
474
682
412
3776
PRE
6
6
299
352
787
571
205
474
682
412
3782
B
Expression
Cell type
pre.L
L
Z
eP
mP
IP
D
MI-II
CCND1
MAD2L1
HERC5
SMC1B
ASAH1
BHMG1
LY6K
DPPA5
MEIOB
ARL6IP1
CALM2
LSM6
MORF4L1
HDGFL1
CETN1
YBX3
RPGRIP1
LUZP2
ENDOG
EFHD1
MRPL28
NPM2
SUN3
CALR3
PDE4A
NRM
C
DMRTB1
HMGN3
SMC1A
MIF
REC114
GPATCH4
SAMD15
MRPS26
STRA8
PRSS50
RAD21L1
BTG3
ADAM2
MLLT10
CCDC38
CCDC85B
SETX
TOP2B
WDR82
C11H14orf39
MISP3
NPM2
INCENP
CCNA1
HSPA2
SELENOW
PEBP1
PSMA8
CCER1
CLDND2
FBXO39
TMEM89
tSNE_2
tSNE_1
Expression
High
Low
Cell type
pre.L
L
Z
eP
mP
IP
D
MI-II
D
Relative Expression
Pseudo-time
Component 2
Component 1

Figure S3. Dynamic gene expression pattern analysis of SPC subsets, related to Figure 3. (A) Balloon plot showing the number of cellular fractions in SPC subsets. (B) Heatmap of normalized expression in the DEGs (Wilcoxon rank sum test, p-value < 0.05) of SPC subsets. (C) Expression patterns of additional markers projected on the tSNE plot. (D) Violin plots, trajectory plots, and pseudotime trajectory expression patterns of additional markers in pre.L, L, Z, eP, mP, lP, D, and MI-II.

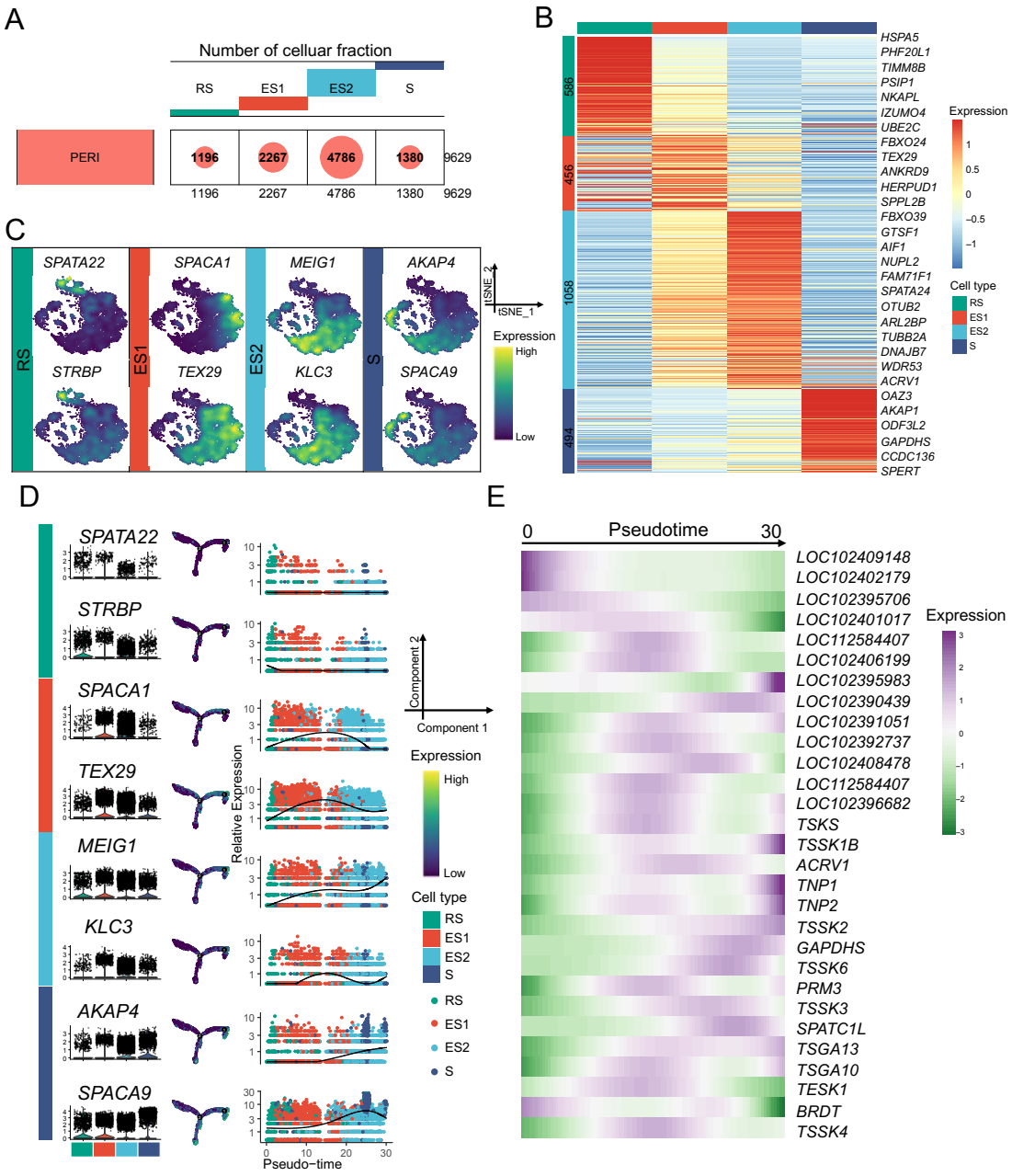

Figure S4. **Dynamic gene expression pattern analysis of Sts subsets, related to Figure 4.** (A) Balloon plot showing the number of cellular fractions in Sts subsets. (B) Heatmap of normalized expression in the DEGs (Wilcoxon rank sum test, p-value < 0.05) of Sts subsets. (C) Expression patterns of additional markers projected on the tSNE plot. (D) Feature plots, trajectory plots, and pseudotime trajectory expression patterns of additional markers in RS, ES1, ES2, and S. (E) Heatmap showing the expression of histone and testis-specific related genes (q-value < 0.01) along the pseudotime axis.

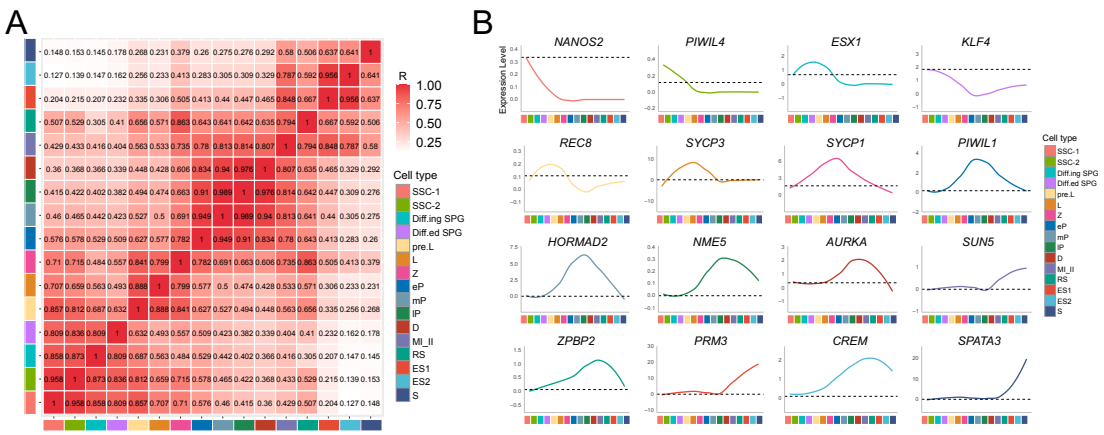

Figure S5. Characterization of buffalo spermatogenic cells. Related to Figure 5. (A) Heatmap of Pearson's correlation coefficient between spermatogenic cells in buffalo. (B) Marker genes expression level of spermatogenic cells.

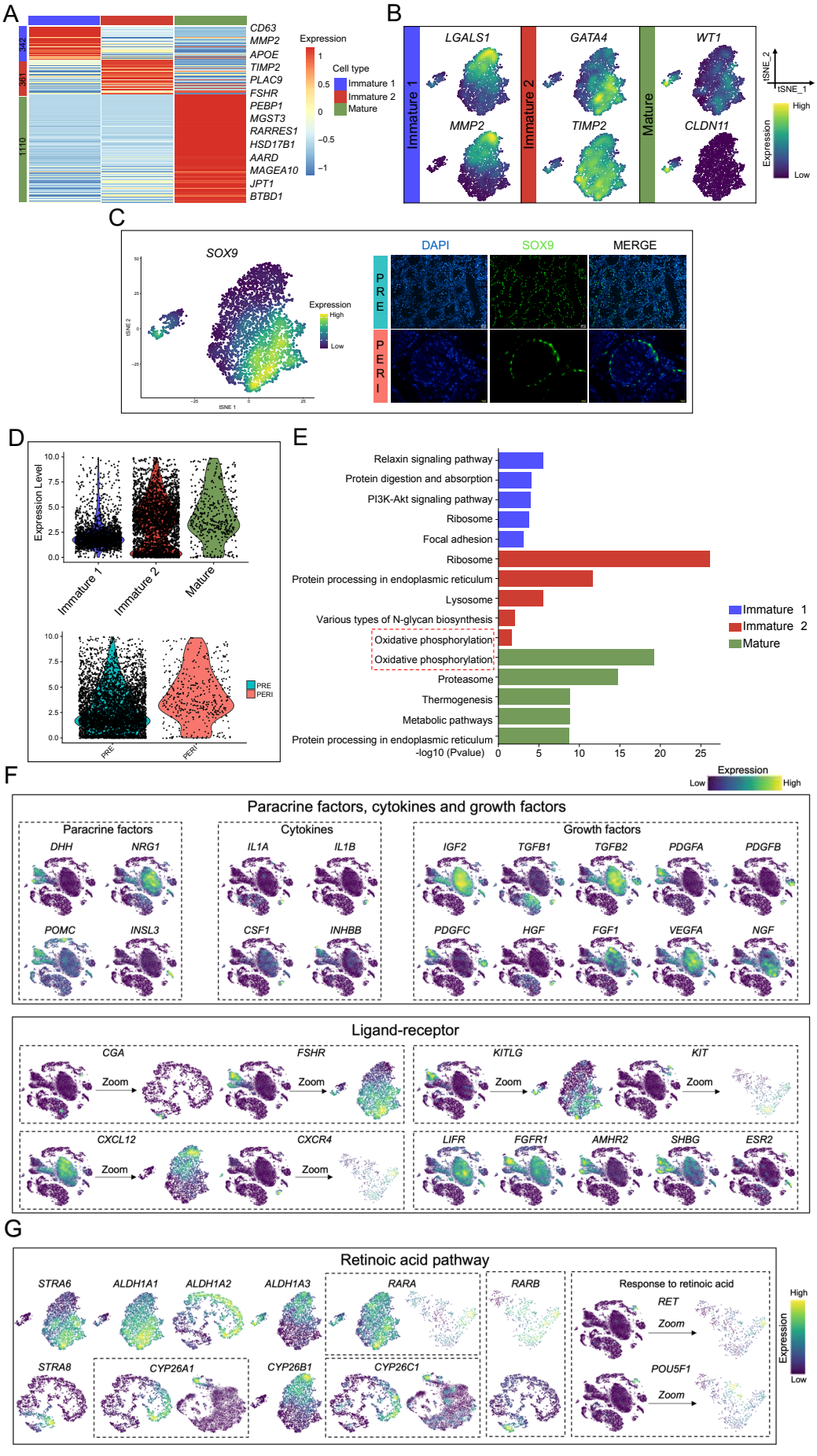
A
342
351
1110
CD63
MMP2
APOE
TIMP2
PLAC9
FSHR
PEBP1
MGST3
RARRES1
HSD17B1
AARD
MAGEA10
JPT1
BTBD1
Expression
1
0.5
0
−0.5
−1
Cell type
Immature 1
Immature 2
Mature
B
Immature 1
Immature 2
Mature
LGALS1
GATA4
WT1
MMP2
TIMP2
CLDN11
tSNE_2
tSNE_1
Expression
High
Low
C
SOX9
Expression
High
Low
tSNE 1
tSNE 2
DAPI
SOX9
MERGE
PRE
PERI
D
Expression Level
10.0
7.5
5.0
2.5
0.0
Immature 1
Immature 2
Mature
PRE
PERI
E
Relaxin signaling pathway
Protein digestion and absorption
PI3K-Akt signaling pathway
Ribosome
Focal adhesion
Ribosome
Protein processing in endoplasmic reticulum
Lysosome
Various types of N-glycan biosynthesis
Oxidative phosphorylation
Oxidative phosphorylation
Proteasome
Thermogenesis
Metabolic pathways
Protein processing in endoplasmic reticulum
-log10 (Pvalue)
0
5
10
15
20
25
Immature 1
Immature 2
Mature
F
Expression
Low
High
Paracrine factors, cytokines and growth factors
Paracrine factors
DHH
NRG1
POMC
INSL3
Cytokines
IL1A
IL1B
CSF1
INHBB
Growth factors
IGF2
TGFB1
TGFB2
PDGFA
PDGFB
PDGFC
HGF
FGF1
VEGFA
NGF
Ligand-receptor
CGA
FSHR
KITLG
KIT
Zoom
CXCL12
CXCR4
LIFR
FGFR1
AMHR2
SHBG
ESR2
G
Retinoic acid pathway
STRA6
ALDH1A1
ALDH1A2
ALDH1A3
RARA
RARB
Response to retinoic acid
RET
POU5F1
Zoom
STRA8
CYP26A1
CYP26B1
CYP26C1
Expression
High
Low

Figure S6. Dynamic gene expression patterns, IF staining, and KEGG enrichment analyses of buffalo somatic lineages, related to Figure 6. (A) Heatmap of normalized expression in the DEGs (Wilcoxon rank sum test, p-value < 0.05) of SCs subsets. (B) Expression patterns of selected markers projected on the tSNE plot. (C) Expression distribution pattern of SOX9 in SCs subsets (left) and IF staining in buffalo testicular paraffin sections (right). Scale bar, 20 μm. (D) Violin plots showing the expression levels of mitochondrial genes in SCs subsets split by cell type (up) and sample (down). (E) Bar plot of the top 5 KEGG pathways (p-value < 0.05) in the enrichment analysis. (F) Global expression patterns of several paracrine factors, cytokines, growth factors, and ligand-receptor pairs. (G) tSNE plot of expression distribution pattern of RA pathway-related genes in individual cell subpopulations.

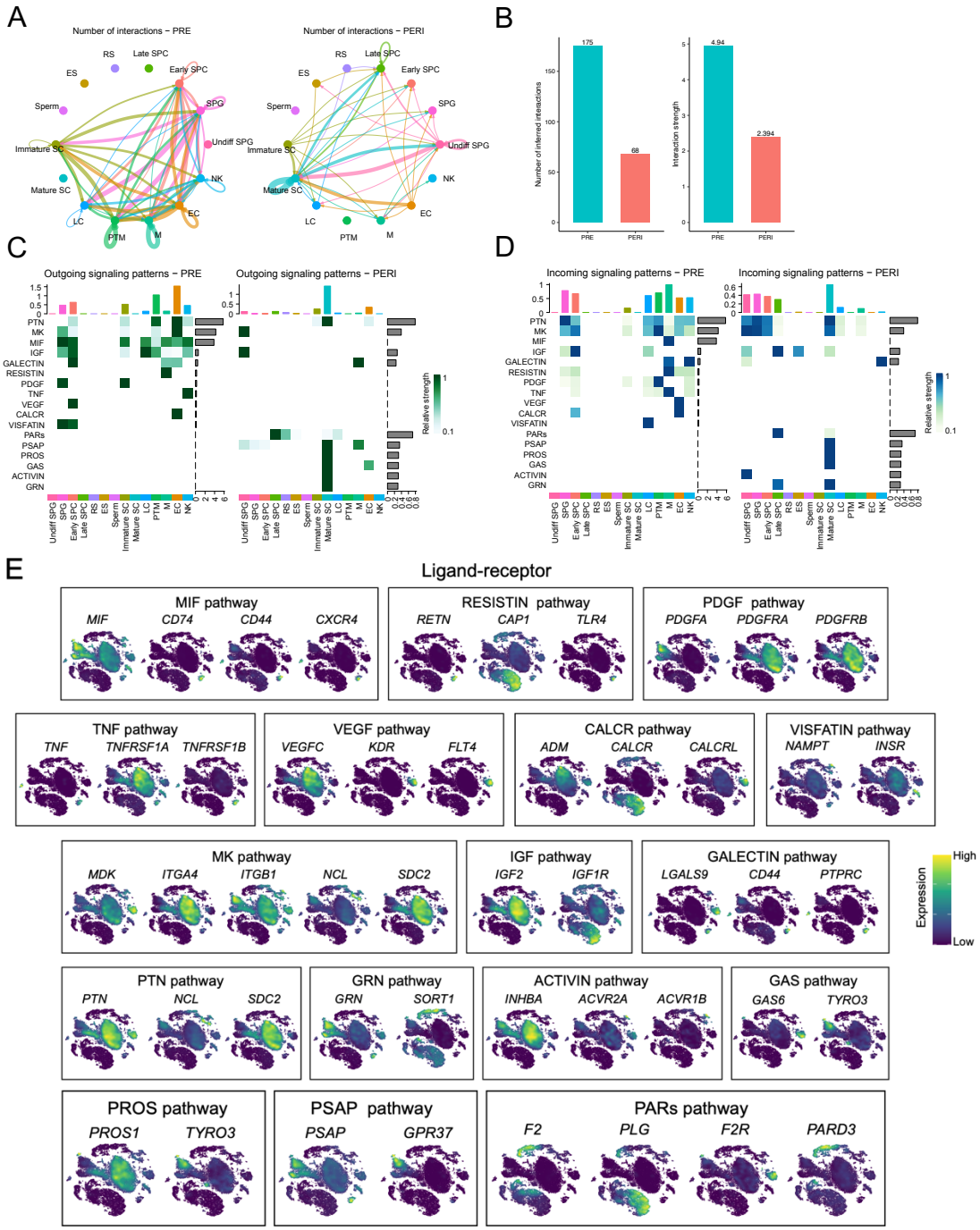

Figure S7. Global landscape of intercellular signaling in buffalo testes, related to Figure 7. (A) The number of interactions and interaction strength among all testicular cell types in PRE (left) and PERI (right). (B) Compare the total number of interactions and interaction strength in PRE (left) and PERI (right). (C) Heatmap comparison of outgoing signaling in PRE- (left) and PERI-derived (right) testicular cells. (D) Heatmap comparison of incoming signaling in PRE- (left) and PERI-derived (right) testicular cells. (E) Expression distribution patterns of ligands-receptors interactions from buffalo testicular cells.